JOURNAL OF SOLID STATE CHEMISTRY **121,** 473–478 (1996)
ARTICLE NO. 0065

Structure Refinement by the Rietveld Method of the Thiogermanates $[(CH_3)_4N]_2MGe_4S_{10}$ (M = Fe, Cd)

O. Achak,* J. Y. Pivan,* M. Maunaye,* M. Loüer,† and D. Loüer†

*Laboratoire de Chimie des eaux et de l'Environnement, ENSC, Campus de Beaulieu, Avenue du Général Leclerc, 35700 Rennes, France; and †Laboratoire de Cristallochimie, URA CNRS 1495, Avenue du Général Leclerc, 35042 Rennes, France

Received June 13, 1995; in revised form October 20, 1995; accepted October 24, 1995

The compounds $[(CH_3)_4N]_2MGe_4S_{10}$ (M = Fe, Cd, Mn, (Co, Mn)) have been synthesized under hydrothermal conditions in glass ampoules at 393 K for two days. They have been investigated by means of thermogravimetry, ionic chromatography, X-ray methods, and IR spectroscopy. They crystallize in the tetragonal symmetry, space group $I\bar{4}$. They are isostructural with $[(CH_3)_4N]_2MnGe_4S_{10}$ and their structures were refined from X-ray powder diffraction intensity data down to the final reliability factors $R_F = 0.07$ ($R_{Bragg} = 0.08$) and $R_F = 0.05$ ($R_{Bragg} = 0.05$) for the Fe and Cd compounds, respectively. The structure consists of tetrahedra sharing apices with a space filling of the covalent (Ge, M)–S framework as small as 45%. The anionic framework generates tunnels with a diameter of about 7 Å, determined from structural results, running along the [100], [010], and [112] directions in which the *TMA* cations are located.

INTRODUCTION

Several inorganic oxides prepared under hydrothermal conditions at low temperature like zeolites, aluminophosphates, molybdenum phosphates, and vanadium phosphates (1, 2) are microporous with internal void volumes up to nearly 40%. Most of these materials contain very complex anionic frameworks which encapsulate inorganic cations (alkaline and alkaline-earth ions) or larger organic tetraalkylammonium cations. These compensating counterions are also structure-directing agents (templating agents) in that they govern, under specific reaction conditions, the void volume and the connectivity between the cavities of the anionic framework.

Relatively little attention has been devoted to similar solids built up from thio or seleno building units (3, 5). Indeed, only very recently, the feasibility of thiogermanates with an S/Ge atomic ratio close to two ($1.8 < S/Ge < 2.2$) has been claimed (5). These compounds were obtained under hydrothermal conditions and the conditions of synthesis together with recent structural investigations have demonstrated the relevant chemical similarities as well as the structural differences of these new compounds with the corresponding microporous oxides (6–8).

The present paper deals with the synthesis and the structure refinement of $TMA_2MGe_4S_{10}$ (M = Fe, Cd). Infrared spectra and thermogravimetric results are discussed and compared with data from related materials.

EXPERIMENTAL DETAILS, STRUCTURE REFINEMENTS AND DISCUSSION

The reactions were carried out in sealed glass ampoules under autogeneous pressure. The reaction of H_2O, freshly prepared amorphous GeS_2, TMACl ($TMA = (CH_3)_4N^+$), NH_4HCO_3, $FeCO_3$ or $CdSO_4$, $\frac{8}{3}$ H_2O introduced in the molar ratio 10:10:5:2:150 for two days at 393 K gave a ca. 60% yield of the corresponding iron and cadmium thiometallogermanates. In the case of TMA_2(Co, Mn)Ge_4S_{10}, the initial reaction mixture was GeS_2, TMACl, NH_4HCO_3, $Co_3(CO_3)(OH)_2$, H_2O, $Mn(CH_3CO_2)_2$, $4H_2O$ in the molar ratios 4:4:2:1:1:120. From our investigations, the molar ratios given above were found to be the optimal ones to obtain the corresponding thiometallogermanates in a reproducible manner. Small amounts of the hexagonal form of GeO_2 were detected as major impurity which could not be eliminated whatever the synthesis conditions in the case of the cadmium compound. The yield of the reactions depends on the total amount of water and the pH value of the starting mixture because of the significant hydrolysis the GeS_2 precursor may undergo. The resulting solids which could also be obtained at room temperature were recovered as powders by filtration and washing with water then dried with ether. The products are different in color, depending upon the outer shell configuration of the d-block element present in the structure; the Cd compound ($4d^{10}$) is white, the Fe compound ($3d^6$) is red–brown, and the dark-green (Co, Mn) compound indicates cobaltous species in tetrahedral environment. SEM photographs from a JEOL JSM 6400 apparatus revealed the Fe powders as tiny tetrahedral-shaped crystals

0022-4596/96 $18.00

TABLE 1
Intensity Data Collection and Crystallographic Data for $TMA_2MGe_4S_{10}$ Compounds

	Mn	Fe	Cd
a(Å)	9.5012(1)	9.4398(3)	9.5387(3)
c(Å)	14.1769(3)	14.1637(7)	14.2963(8)
c/a	1.492	1.500	1.498
V(Å^3)	1282.3	1262.1	1300.8
Space group		$I\bar{4}$	
Angular range (2θ)	10–100	10–70	10–100
Reflections in refinement	354	149	359
Variable parameters	36	28	28
Atoms in asymmetric unit		9	
$R_F = \Sigma \lvert I(\text{“obs”})^{1/2} - I(\text{calc})^{1/2}\rvert / \Sigma I(\text{“obs”})^{1/2}$	0.05	0.07	0.05
$R_B = \Sigma \lvert I(\text{“obs”}) - I(\text{calc})\rvert / \Sigma I(\text{“obs”})$	0.05	0.08	0.05
$R_P = \Sigma \lvert y_i(\text{obs}) - (1/c)\, y_i(\text{calc})\rvert / \Sigma y_i(\text{obs})$	0.05	0.06	0.09
$R_{wP} = \{\Sigma \omega_i [y_i(\text{obs}) - (1/c)\, y_i(\text{calc})]^2 / \Sigma \omega_i [y_i(\text{obs})]^2\}^{1/2}$	0.07	0.08	0.12
GoF	2.22	4.93	4.23

with maximum size about 1 μm. These crystals were intergrown due to the high reaction rates and single crystals of sufficient size could not be recovered for intensity data collection. High-resolution X-ray powder diffraction intensity measurements were recorded on a Siemens D-500 diffractometer using a monochromated source ($\lambda \text{Cu}K_{\alpha 1} = 1.54059$ Å). The diffraction intensity data were collected over the angular range $10° < 2\theta < 100°$ with an angular step size of 0.02° (2θ) and the respective counting times of 55 seconds and 27 seconds per point for $TMA_2FeGe_4S_{10}$ and $TMA_2CdGe_4S_{10}$. The auto-indexing program DICVOL91 (9) gave centered tetragonal unit cells with the lattice parameters $a = 9.4315(2)$ Å, $c = 14.1533(5)$ Å for the iron compound and $a = 9.5386(4)$ Å, $c = 14.2962(4)$ Å for the cadmium compound with a quasi-constant c/a ratio. The significant broadening of the peaks for the thiometallogermanate phases with respect to the GeO_2 impurity must be attributed to size effects in that the halfwidth of the peaks systematically increases as the diffraction angle increases. This induces less accurate measurements in the high part of the diffraction patterns. In addition to the size effects, some fluorescence screens the lowest intensity data for the Fe compound. The crystallographic data, intensity data collection, and refinement conditions are listed in Table 1. Rietveld refinements of the Fe and Cd structures were performed using the Rietveld program FULLPROF (10) with the atomic coordinates of $TMA_2MnGe_4S_{10}$ as starting parameters (8). The positional and thermal parameters of the heaviest atoms (Ge, M, and S) were refined. An overall temperature factor was refined for the lighter atoms and constraints were applied to the carbon atoms of the TMA groups (same coordinates as in $TMA_2MnGe_4S_{10}$). The reliability factors (profile factors and structural factors) for each structure are given and compared to those previously reported for the isostructural compound $TMA_2MnGe_4S_{10}$ in Table 1. Observed and calculated X-ray powder diffraction patterns are shown in Fig. 1 and the structure is given in Fig. 2. The final atomic coordinates and temperature factors are listed in Table 2. Selected interatomic distances and bond angles are listed in Table 3 and compared with those obtained for $TMA_2MnGe_4S_{10}$. Although the bond distances and angles are less accurate for the two structures described herein, all the values agree well with interatomic distances and bond angles reported in previous studies for similar building units (11–15).

The structural analysis reveals an extended 3D anionic framework $MGe_4S_{10}^{2-}$ based upon interconnected tetrahedral units “MS_4” and “Ge_4S_{10}.” The interatomic distances within the thioanion are indicative of covalency. The “Ge_4S_{10}” units do not exhibit appreciable change compared to the structural features known for such tetrahedral blocks in $M_xGe_4S_{10}$ ($M^+ = Na^+$, Tl^+, Cs^+, Ba^{2+}, TMA^+) (11–15). The M–S bond distances in the MS_4 tetrahedra are normally increasing as the polarizing power of the M element is decreasing. The S_2–M–S_2 bond angles show that the M centers are significantly deviating from the ideal Td symmetry. The MS_4 tetrahedra are flattened along the [001] direction and do not posses yet threefold axes. As a result, four bond angles are larger than the expected values for tetrahedral coordination and two are smaller. The angular deformation is concerted within the MS_4 units since the average value of the S–M–S bond angle is close to 109° for each compound (Table 3). The resulting 3D anionic framework generates large interconnected tunnels running along the [010], [100], and [112] directions. These tunnels are filled up in an ordered manner by the organic cations TMA^+. No distances shorter than 3.75 Å occur between the TMA groups and the framework.

INFRARED AND THERMOGRAVIMETRIC ANALYSES

Infrared absorption spectra have been recorded for each compound on a Nicolet apparatus within the wavenumber range 80–500 cm^{-1} and a resolution of 4 cm^{-1}. The samples were pelletized in a polyethylene matrix. The main vibrational lines are reported in Table 4 and the spectra are shown in Fig. 3. Vibrational modes of the MS_4 tetrahedra are superimposed to the bands of the Ge_4S_{10} units which explains that additional lines are present in the spectra of the thiometallogermanates with respect to the spectrum of $TMA_4Ge_4S_{10}$. In the light of the literature, very few accurate IR data are known for sulfur-containing com-

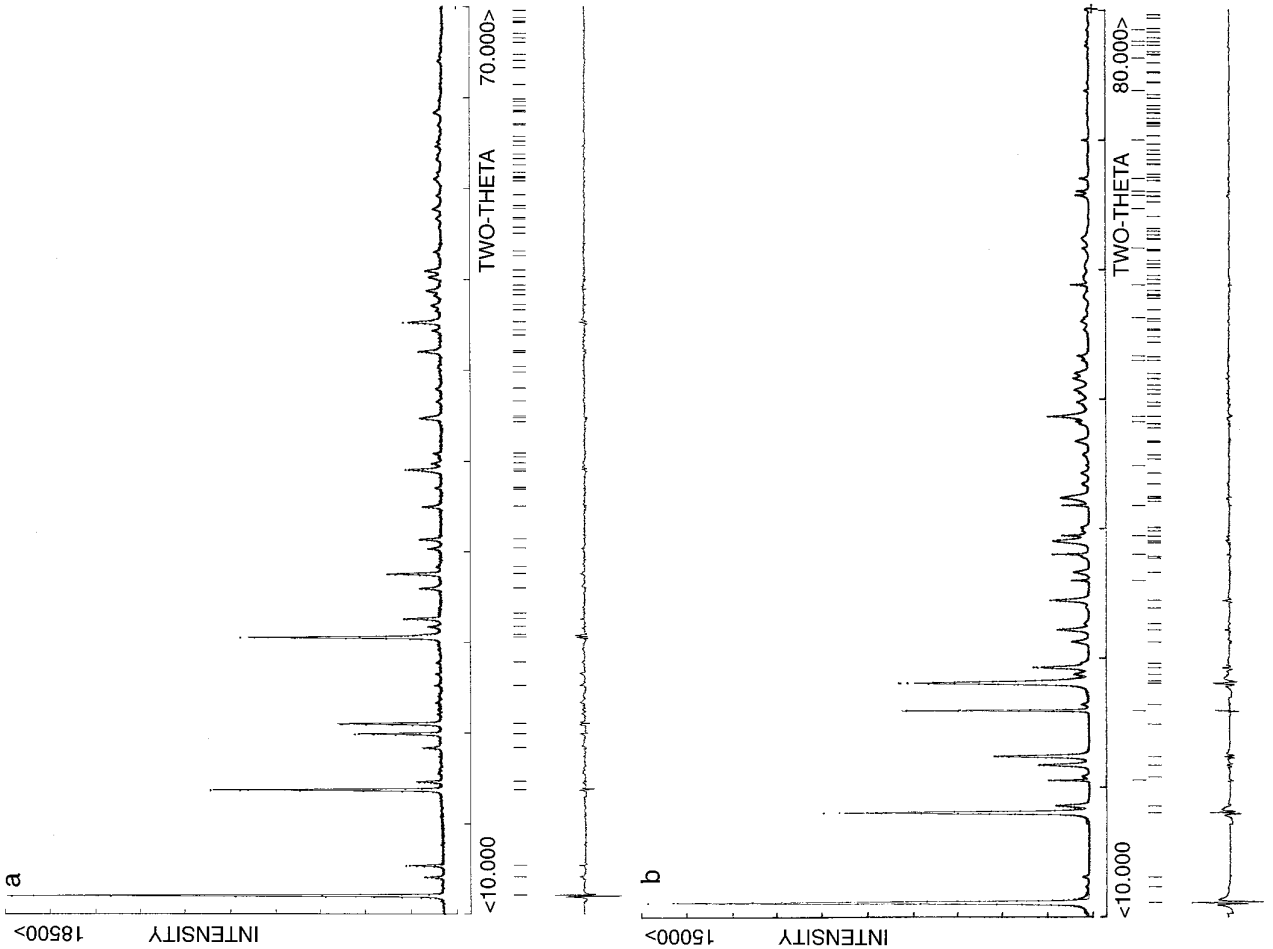

FIG. 1. The final Rietveld plot for $TMA_2FeGe_4S_{10}$ (a) and $TMA_2CdGe_4S_{10}$ (b) from monochromatic X-ray powder diffraction. (Upper trace) Observed data as dots, calculated patterns as solid lines. (Lower trace) Plot of the difference observed minus calculated.

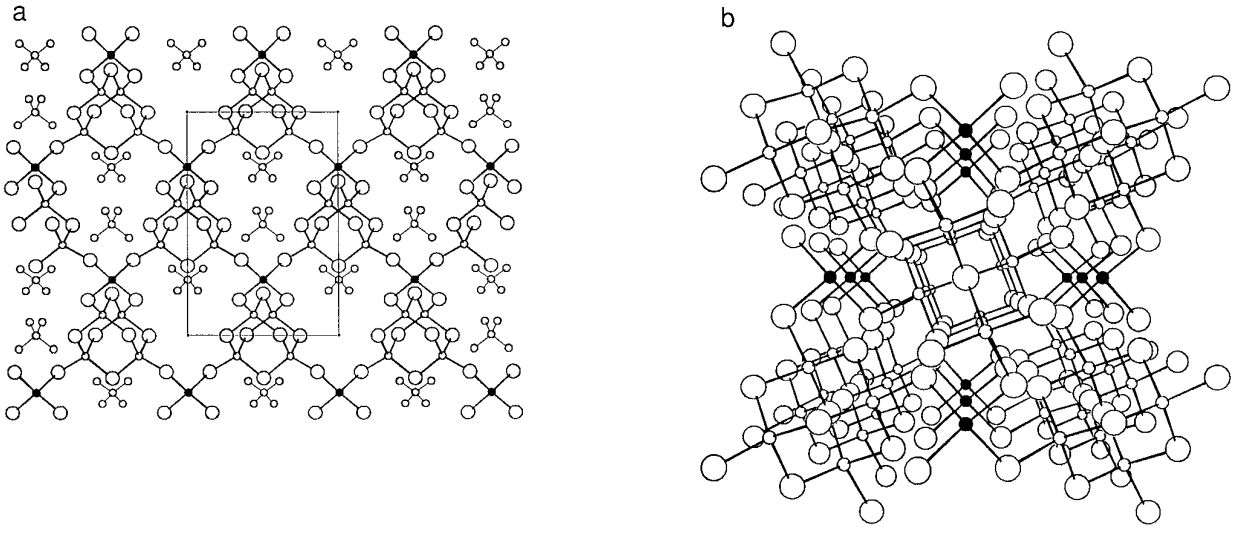

FIG. 2. Views of the structure of $TMA_2MGe_4S_{10}$: (a) view along the [100] direction showing the channels. The *TMA* groups are located in the channels. Large circles, S atoms; medium circles, Ge atoms; and shaded circles, *M* atoms. (b) View along along the [001] direction. The *TMA* groups are not shown for clarity. Large circles, S atoms; medium circles, Ge atoms; and shaded circles, *M* atoms.

pounds. IR spectra have been reported for $M_xGe_4S_{10}$ solids (11–15) with isolated Ge_4S_{10} units in good agreement with the spectrum of $TMA_4Ge_4S_{10}$ and only one theoretical study in the Td point group has been made on related compounds (16). Thus, some difficulties appear to assign the different bands of the thiometallogermanates reported here. However, according to the structure determination and previous studies (15, 17), the Ge–S vibrational modes are mainly responsible for the bands around 400, 320, 280, and 200 cm^{-1}, and the wide band around 250 cm^{-1} can be attributed to *M*–S vibrations. An exact assignment of the bands requires a complex theoretical study which in turn requires a detailed model of the force field in these compounds. Thus, although exact assignments cannot be made, the obtained IR spectra provide useful and qualitative information in that there is close connection between the IR spectra and the structure type.

In addition, all the compounds $TMA_2MGe_4S_{10}$ (*M* = Mn, Fe, Cd, (Co, Mn)) have been analyzed by using a RIGAKU PTC-10A thermogravimetric analyzer. The thermogravimetric curves for each compound heated at 10°C/min. up to 600°C in air are shown in Fig. 4. With the exception of $TMA_2MnGe_4S_{10}$, all compounds contain water molecules with a water loss of about 5% for Fe and Cd compounds and 10% for the mixed TMA_2(Co, Mn)Ge_4S_{10}. The T_{onset} close to 100°C for each compound indicates that these water molecules are weakly bonded. Furthermore, these thermogravimetric data compared to

TABLE 2
Atomic Coordinates and Isotropic Temperature Factors with Their e.s.d's[a]

	$TMA_2FeGe_4S_{10}$				$TMA_2CdGe_4S_{10}$			
	x	*y*	*z*	*B* ($Å^2$)	*x*	*y*	*z*	*B* ($Å^2$)
M	0.5	0	0.25	1.4(3)	0.5	0	0.25	2.6(2)
Ge	0.4368(9)	0.3232(7)	0.0904(5)	0.9(3)	0.4293(5)	0.3290(4)	0.0896(3)	1.6(2)
S_1	0.256(2)	0.389(1)	−0.003(1)	3.9(4)	0.253(1)	0.398(1)	−0.006(1)	4.9(2)
S_2	0.342(2)	0.143(1)	0.159(1)	3.9(4)	0.329(1)	0.159(1)	0.167(1)	4.9(2)
S_3	0.5	0.5	0.186(2)	3.9(4)	0.5	0.5	0.182(2)	4.9(2)
N_1	0	0	0		0	0	0	
N_2	0	0.5	0.25		0	0.5	0.25	
C_1	0.115	0.041	−0.059		0.115	0.041	−0.059	
C_2	−0.067	0.397	0.200		−0.067	0.397	0.200	

[a] B_{iso} were constrained to be the same for S atoms. The atomic coordinates of C atoms were constrained to be the same as in the structure of $TMA_2MnGe_4S_{10}$ (8). For C and N atoms an overall *B* parameter (0.86 $Å^2$ for $TMA_2FeGe_4S_{10}$ and 0.48 $Å^2$ for $TMA_2CdGe_4S_{10}$) was refined.

TABLE 3
Interatomic Bond Distances (Å) and Angles (°) with Their e.s.d.'s

		$TMA_2MnGe_4S_{10}$	$TMA_2FeGe_4S_{10}$	$TMA_2CdGe_4S_{10}$
Ge	$-S_1$	2.246(7)	2.24(1)	2.25(1)
	$-S_1$	2.178(7)	2.15(1)	2.17(1)
	$-S_2$	2.173(7)	2.15(1)	2.18(1)
	$-S_3$	2.262(6)	2.23(1)	2.20(1)
M	$-S_2$	2.459(6)	2.39(1)	2.51(1)
S_1-Ge-S_1		110.3(6)	108.7(9)	109.2(8)
S_1-Ge-S_2		100.0(6)	99.8(9)	101.4(8)
S_1-Ge-S_2		111.2(5)	110.3(9)	111.2(8)
S_2-Ge-S_3		111.1(4)	115.4(9)	112.7(7)
S_1-Ge-S_3		111.4(5)	110.5(9)	111.8(8)
S_1-Ge-S_3		112.2(5)	111.5(9)	110.3(8)
$Ge-S_1-Ge(\times4)$		107.4(4)	109.3(9)	107.9(6)
$Ge-S_3-Ge(\times2)$		102.9(6)	105.2(8)	106.5(5)
$Ge-S_2-M$		112.8(2)	115.5(9)	114.3(6)
$S_2-M-S_2(\times4)$		103.7(4)	106.9(9)	103.1(7)
$S_2-M-S_2(\times2)$		121.7(6)	114.6(9)	123.3(8)

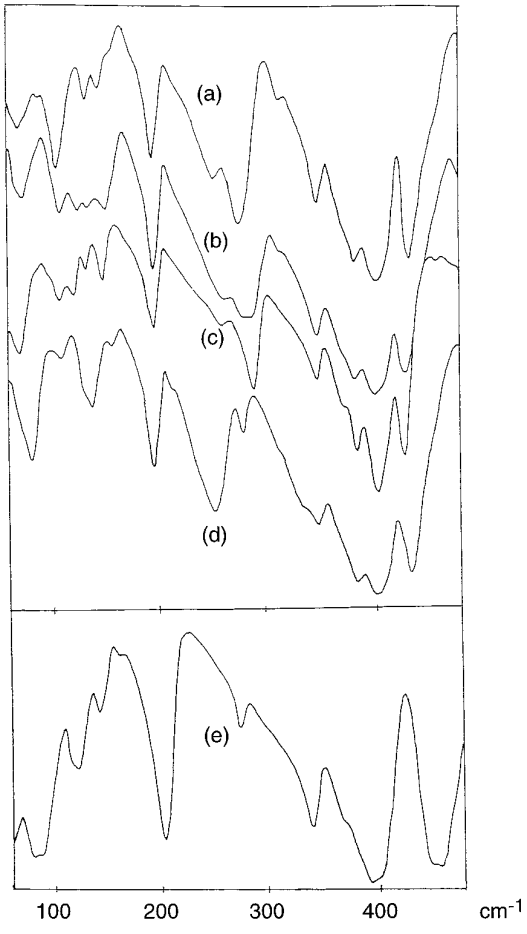

FIG. 3. Infrared spectra for (a) $TMA_2MnGe_4S_{10}$, (b) $TMA_2(Co, Mn)Ge_4S_{10}$, (c) $TMA_2FeGe_4S_{10}$, (d) $TMA_2CdGe_4S_{10}$, and (e) $TMA_4Ge_4S_{10}$.

the structural results show that these water molecules, not located during the structure refinements, are presumably disordered in the channels. Upon heating, the water-free compounds exhibit different behaviors. The shapes of the Δm versus T curves are dependent on the nature of the incorporated divalent M^{II} element. The sharp weight loss of about 20–23 wt% in one step occuring at 330 and 230°C for the Mn and Fe derivatives, respectively, is unambiguously attributed to the degradation of the occluded organic templates. From structural results, the tetramethylammonium cations are almost equivalent and weakly bonded to the $MGe_4S_{10}^{2-}$ anionic framework according to bond length calculations, so the gap of 100°C in the degradation temperature of the organic species must be ascribed to a large extent to the nature of the divalent element present in the structure. These thermogravimetric data suggest that the degradation products are not the same for the iron and the manganese compounds. The thermogravimetric analysis of the Cd and (Co, Mn) derivative compounds shows that the degradation of the TMA^+ cations occurs in two more or less marked steps. The first step around 230°C, well defined in the case of $TMA_2(Co, Mn)Ge_4S_{10}$, is reminiscent of the data for the iron compound while the second step at higher temperature must be compared to the data for the manganese compound. Similar results have been already reported for related microporous oxide materials such as M^{III}-substituted zeolites with $Pr_{4-x}NH_x^+$ occluded templates (17). From these studies, different degradation products were evidenced in relation with the M^{III} element which suggested that the initial decomposition mechanism was mainly the Hoffman elimination reaction followed by β-eliminations. Whatever the mechanism involved in the template degradation, the total weight loss of about 23% in good agreement with the structural results shows that

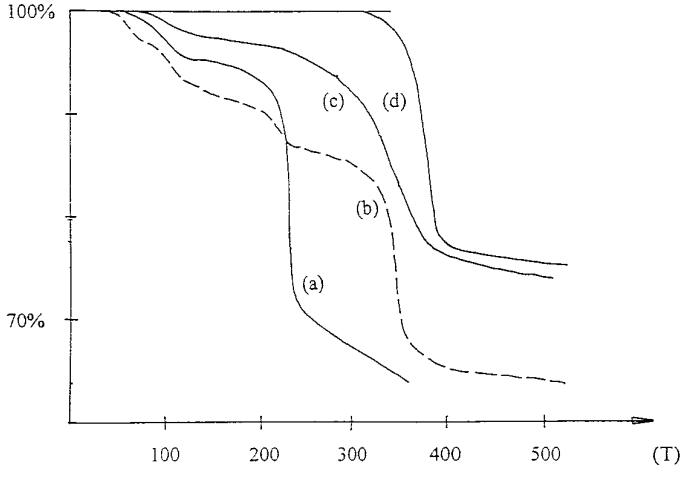

FIG. 4. TG curves for samples $TMA_2MGe_4S_{10}$ (heating rate 10°C min^{-1} in air): (a) M = Fe, (b) M = (Co, Mn), (c) M = Cd, and (d) M = Mn.

TABLE 4
Infrared Lines (cm^{-1}) for the $TMA_2MGe_4S_{10}$ Compounds

$TMA_2MnGe_4S_{10}$	$TMA_2FeGe_4S_{10}$	$TMA_2CdGe_4S_{10}$	$TMA_2AGe_4S_{10}$[a]	$TMA_4Ge_4S_{10}$
71	71	81	74	80
	100			89
108	110	110	110	
	123	132 sh.	127	122
135	136	140	136	144
148				
155	151	159	154	163
177				
198	198	197	197	202
	232 sh.	218 sh.		
255	255	253	263	
279	279	281	283	274
	290		291 sh.	
312		315 sh.	315 sh.	
		336 sh.		341
350	348	349	350	
	368 sh.			368 sh.
384	383	384	383	392
402	399	401	400	400
435	425	436	429	
	460			451
	473 sh.			459

[a] A = (Co, Mn) and sh. means shoulder.

no additional organic species are present in the structures described herein. Taking into account all of these data, it is likely that at least two different mechanisms, not yet elucidated, occur during the template degradation. Further thermogravimetric investigations coupled to mass spectroscopy and (or) gas chromatography would be of great interest in order to understand the mechanisms during the degradation in that one can expect different chemical or catalytic properties in the template-free compounds in relation to the divalent metal in the structure.

REFERENCES

1. R. M. Barrer, "Hydrothermal Synthesis of the Zeolites," Academic Press, London, 1982, and references therein.
2. R. C. Haushalter and L. A. Mundi, *Chem. Mater.* **4,** 31 (1992), and references therein.
3. J. B. Parise, *Science* **251,** 293 (1991).
4. S. Dinghra and M. G. Kanatzidis, *Science* **258,** 1769 (1992).
5. R. L. Bedard, S. T. Wilson, L. D. Vail, J. M. Bennett, and E. M. Flanigen, *in* "Zeolites: Facts, Figures, Future" (P. A. Jacobs and R. A. Van Santen, Eds.), p. 375, Elsevier, Amsterdam, 1989.
6. O. Achak, J. Y. Pivan, and M. Maunaye, *in* "Proceedings of 10e Réunion du Groupe Français des Zéolites, Dijon, Mar. 1994."
7. O. M. Yaghi, Z. Sun, D. W. Richardson, and T. L. Roy, *J. Am. Chem. Soc.* **116,** 807 (1994).
8. O. Achak, J. Y. Pivan, M. Maunaye, M. Louër, and D. Louër, *J. Alloys Compd.* **219,** 111 (1995).
9. A. Boultif and D. Louër, *J. Appl. Crystallogr.* **24,** 987 (1991).
10. J. Rodriguez-Carvajal, *in* "Collected Abstracts of Powder Diffraction Meeting, Toulouse, 1990."
11. E. Philippot, M. Ribes, and O. Lindqvist, *Rev. Chim. Miner.* **8,** 477 (1971).
12. E. Philippot, M. Ribes, and J. Ollivier-Fourcade, *J. Solid State Chem.* **33,** 155 (1975).
13. S. Pohl and B. Krebs, *Z. Anorg. Allg. Chem.* **424,** 265 (1976).
14. G. Eulenberger, *Acta Crystallogr. Sect. B* **32,** 3059 (1976).
15. J. Y. Pivan, O. Achak, M. Louër, and D. Louër, *Chem. Mater.* **6,** 808 (1994).
16. A. Muller, B. N. Cyvin, S. J. Cyvin, S. Pohl, and B. Krebs, *Spectrochim. Acta Part A* **32,** 67 (1976).
17. M. Ribes and M. Maurin, *Rev. Chim. Miner.* **7,** 75 (1970).
18. S. Bilger, M. Soulard, H. Kessler, and J. L. Guth, *Zeolites* **11,** 784 (1991).